Supporting Information for

Interactions between Hofmeister Anions and the Binding Pocket of a Protein

Jerome M. Fox[a], Kyungtae Kang[a], Woody Sherman[b], Annie Héroux[c], Madhavi Sastry[b], Mostafa Baghbanzadeh[a] , Matthew R. Lockett[a], and George M. Whitesides[a*]

[a] *Department of Chemistry and Chemical Biology, Harvard University*

12 Oxford Street, Cambridge, MA 02138

[b] *Schrödinger, Inc.,*

120 West 45th Street, New York, NY 10036-4041

[c] *National Synchrotron Light Source, Photon Sciences Directorate*

* To whom correspondence may be addressed: gwhitesides@gmwgroup.harvard.edu

This PDF File includes:
SI Methods
SI Appendices 1-4
SI Figures 1-7
SI Tables 1-7

SI Methods

Purification of Human Carbonic Anhydrase II (HCAII). We overexpressed HCAII in BL21(DE3)pLysS competent cells (Promega) via a pACA plasmid (a kind gift from Fierke and coworkers); this plasmid contains the gene for HCAII under control of the lac operon. We purified HCAII according to the procedure described by Fierke and coworkers.[1]

Synthesis of Ligands. We synthesized benzo[*d*]thiazole-2-sulfonamide (**BTA**) according to previously published synthetic procedures.[2] We stored solid BTA under vacuum at room temperature.

Isothermal Titration Calorimetry (ITC). We carried out all ITC experiments in a Microcal Auto ITC (GE Healthcare) in 10 mM sodium phosphate buffer (*pH* 7.6, 1% DMSO) at 298.15 K. Experiments consisted of 20 injections (8.02 μL) of **BTA** (100 μM) into a solution of 5 μM HCAII (sodium salts, when present, were present at a concentration of 100 mM in both ligand and protein solutions). We used an injection interval of 300 seconds, a stirring speed of 300 rpm, and a reference power of 14 μcal/sec. Using Origin 7.0, we estimated K_a and $\Delta H°_{bind}$ by using a nonlinear fit to a single-site model (Table S1). We then converted these observed values to those corresponding to the association of Ar-SO_2-NH^- and HCAII-OH_2^+ to form HA-Zn^{2+}-$NHSO_2$-Ar by following the procedure outlined by Snyder et al.[2] (Table S2). All experimentally determined values of K_a, $\Delta H°_{bind}$, $-T\Delta S°_{bind}$, and $\Delta G°_{bind}$ represent averages of at least seven separate experiments (Tables S1-S2).

We note, the procedure outlined by Snyder et al.[2] requires knowledge of both the pK_a of the sulfonamide group of **BTA** (i.e., the pK_a corresponding to the dissociation of Ar-SO_2-NH_2 to

Ar-SO_2-NH^- and H^+) and the pK_a of HCAII-OH_2^+ (i.e., the pK_a corresponding to the dissociation of HCAII-OH_2^+ to HCAII-OH and H^+). In contrast with the pK_a for the dissociation of HCAII-OH_2^+ (where species with +1 charges exist before and after dissociation), the pK_a for the dissociation of **BTA** (where charged species exist only after deprotonation of the sulfonamide) is sensitive to ionic strength. Accordingly, we estimated the pK_a of the sulfonamide group of **BTA** in the presence of each sodium salt (i.e., a 10 mM of sodium phosphate buffer with 100 mM of a specific sodium salt) by using Eq. S1.

$$pK'_{a,100} = pK'_a + \log\left(\frac{g^+_{100} \cdot g^-_{100}}{g^+ \cdot g^-}\right) \quad \text{(S1)}$$

where

$$\log(g) = -\frac{0.5 \times (Z_i)^2 \times \sqrt{I}}{1 + \sqrt{I}} \quad \text{(S2)}$$

and

$$I = \frac{1}{2} \times \sum_{i=1}^{n} c_i \times Z_i^2 \quad \text{(S3)}$$

In Equation S1, pK_a' is the pK_a of the sulfonamide group of **BTA** in 10 mM sodium phosphate buffer (pK_a' = 8.2 as determined by Breiten et al.[3]), $pK'_{a,100}$ is the pK_a of the sulfonamide group of **BTA** in 10 mM sodium phosphate buffer with 100 mM of a specific sodium salt, γ^+ and γ^- are the activity coefficients for ions with +1 and -1 charges, respectively, in 10 mM sodium phosphate buffer, γ^+_{100} *and* γ^-_{100} are the activity coefficients for ions with +1 and -1 charges, respectively, in 10 mM sodium phosphate buffer with 100 mM of a specific sodium salt, I is the ionic strength of the buffer, and Z_i and c_i are the charge and valence, respectively, of species i in the buffer. The speciation of anions in buffers containing Na_2HPO_4, $NaCH_3COO^-$, and $NaHCO_3$, at *pH* 7.6 was estimated using pK_a values reported by Goldberg et al.[4] Equations S1-S3 are

further elaborated by Stumm and Morgan[5]. Values of pK_a and I for each buffer condition are reported in Table S3.

For all experiments, we used the following stock solutions of reagents: 20 mM **BTA** (DMSO), 2 M sodium salt (in 10 mM sodium phosphate buffer, *pH* 7.6), and 100-200 μM HCAII (10 mM sodium phosphate buffer, *pH* 7.6). Solutions of sulfate were prepared with a disodium salt; solutions of phosphate, with a combination of monosodium and disodium salts to yield a buffer with *pH* = 7.6. All other solutions were prepared with monosodium salts. In the Main Text and Supporting Information, all sodium salts are annotated with the dominant anion present in solution at *pH* = 7.6. To ensure accurate determination of the concentration of protein in the HCAII stock solution, we carried out the following steps: (i) we estimated the concentration of HCAII by measuring the absorbance of the stock solution at 280 nm (the extinction coefficient for HCAII: 50,700 cm^{-1} M^{-1}), (ii) we corrected the estimated concentration by carrying out 7 ITC experiments with a standard methazolamide solution (for which the concentration was determined using NMR).

Errors associated with measurements of $\Delta H°_{bind}$ and K_a translate to errors in estimates of $\Delta S°_{bind}$ and $\Delta G°_{bind}$ and thereby cause *H/S* compensation to be perceived where it does not occur.[6] To reduce such errors, we carried out the following steps: (i) we compared the binding stoichiometry of **BTA** with the methazolamide standard to obtain an accurate concentration of **BTA** in the stock solution; (ii) we determined the concentration of active protein before and after each set of seven runs by measuring $\Delta H°_{bind}$ and K_a of a standard sulfonamide (methazolimide) for which the concentration had been determined accurately with NMR; (iii) we used identical stock solutions of **BTA** for each experiment, thereby eliminating changes in the concentration of **BTA** between experiments; and (iv) we used seven separate ITC runs to measure enthalpies of binding ($\Delta H°_{bind}$) and association constants (K_a) for **BTA** in the presence of each anion.

The Competition Assay. We estimated thermodynamic parameters for the binding of anions to the Zn^{2+} cofactor (the formation of ion pairs between anions and Zn^{2+}) by following the method developed by Zhang et al to measure binding parameters for low-affinity inhibitors.[7] Briefly, in the presence of a low-affinity inhibitor (an anion from the Hofmeister series, Figure 1A), the observed dissociation constant ($K_{d,BTA}^{obs}$) and enthalpy of binding ($\Delta H^{\circ}{}_{bind,BTA}^{obs}$) of a high-affinity inhibitor (**BTA**) differ from values of the dissociation constant ($K_{d,BTA}$) and enthalpy of binding ($\Delta H^{\circ}_{bind\text{-}BTA}$) determined in the absence of ions in accordance with Eqs. 1 and 2, where $K_{d,anion}$ and $\Delta H^{\circ}_{bind,anion}$ are the dissociation constant and enthalpy of binding, respectively, for a specific anion, and $[A_{tot}]$ is the total concentration of that anion.

$$K_{d,BTA}^{obs} = K_{d,BTA} + \frac{K_{d,BTA}}{K_{d,anion}}\left[A_{tot}\right] \tag{1}$$

$$\Delta H_{bind,BTA}^{obs} = \Delta H_{bind,BTA}^{\circ} - \frac{\Delta H_{bind,anion}^{\circ}}{1 + \frac{K_{d,anion}}{\left[A_{tot}\right]}} \tag{2}$$

(We note, $K_{d,BTA}^{obs}$, $\Delta H^{\circ}{}_{bind,BTA}^{obs}$, $K_{d,BTA}$, and $\Delta H^{\circ}_{bind\text{-}BTA}$ in Eqs. 1 and 2 represent the pK_a-corrected binding parameters, calculated as described above; "observed," in the context of Eqs. 1 and 2 does not correspond to "measured" thermodynamic parameters, but rather to the pK_a-corrected thermodynamic parameters estimated under the assumption that anions do not act as inhibitors). Equations 1 and 2 can be rearranged to give equations describing the dissociation constant and enthalpy of binding of the low-affinity inhibitor in terms of measureable parameters:

$$K_{d,anion} = \frac{[A_{tot}]\cdot K_{d,BTA}}{K_{d,BTA}^{obs} - K_{d,BTA}} \tag{S4}$$

$$\Delta H^{\circ}{}_{bind,anion} = \left(\Delta H^{\circ}{}_{bind,BTA} - \Delta H^{\circ}{}_{bind,BTA}^{obs}\right) \cdot \left(1 + \frac{K_{d,anion}}{[A_{tot}]}\right) \tag{S5}$$

Using equations S4 and S5, we estimated the dissociation constant ($K_{d,anion}$ and $\Delta H°_{bind,anion}$) for each anion; from these values, we estimated $\Delta G°_{bind,anion}$ and $-T\Delta S°_{bind,anion}$ (Table S4). Reported uncertainties in values of $K_{d,anion}$, $\Delta H°_{bind,anion}$, $\Delta G°_{bind,anion}$, and $-T\Delta S°_{bind,anion}$ represent error propagated from standard errors (n ≥ 7) of values of $K_{d,BTA}^{obs}$, $\Delta H°_{bind,BTA}^{obs}$, $K_{d,BTA}$, and $\Delta H°_{bind-BTA}$.

We note, the value of $K_{d,BTA}^{obs}$ determined in the presence of 100 mM Na_2HPO_4 is statistically indistinguishable (P<0.01) from the value of $K_{d,BTA}^{obs}$ determined in the absence of sodium salts. This result suggests that the higher ionic strength of the 10 mM sodium phosphate buffer containing 100 mM Na_2HPO_4 (relative to the ionic strength of the 10 mM sodium phosphate buffer with no sodium salts added; see Table S3) had a negligible influence on the thermodynamics of **BTA**-HCAII association.

The value of $K_{d,BTA}^{obs}$ determined in the presence of 100 mM Na_2SO_4, by contrast, is lower than the value of $K_{d,BTA}^{obs}$ determined in the absence of sodium salts. This lower value of $K_{d,BTA}^{obs}$ likely results from either (i) the tendency of Na_2SO_4 to reduce the solubility of BTA and, thus, to make the process of BTA desolvation more free energetically favorable or (ii) measurement error. As solution calorimetry suggests that 100 mM Na_2SO_4 has a negligible influence on the solubility of BTA in aqueous solution (see below), the latter seems the most likely cause.

To summarize, under the conditions of our experiments, we could not estimate the thermodynamic parameters describing the binding of SO_4^- or HPO_4^{2-} to the Zn^{2+} cofactor of HCAII (i.e., the heat signal caused by the binding of these anions to Zn^{2+} was small compared to small variations in signal from experiment to experiment).

Thermodynamic Parameters for the Partitioning of Ligands from Buffer to Octanol. In the competition assay, Eqs. 1 and 2 are valid only if the intrinsic thermodynamics of BTA binding to

HCAII remains unchanged in the presence of sodium salts. To ensure that Hofmeister anions, which are known to alter the solubility of hydrocarbons,[8] do not alter the thermodynamics of **BTA** desolvation, we estimated the free energy ($\Delta G°_{ow}$), enthalpy ($\Delta H°_{ow}$), and entropy ($-T\Delta S°_{ow}$) of partitioning from buffer to octanol for **BTA** (the protonated form) in the presence (and absence) of seven sodium salts with anions spanning the Hofmeister series (Na_2SO_4, Na_2HPO_4, NaCl, NaBr, NaI, $NaClO_4$, NaSCN).

To estimate $\Delta G°_{ow}$, we carried out the following steps: (i) we diluted **BTA** to a concentration of 200 μM in 4 mL of buffer-saturated octanol, added 4 mL of octanol-saturated buffer (10 mM, *pH* 7.8, 100 mM sodium salt), and mixed for at least 24 hours (20 mL scintillation vials); (ii) we measured the concentration of **BTA** in the octanol and buffer phases ($[Ar\text{-}SO_2NH_2]_O$ and $[Ar\text{-}SO_2NH_2]_W$, respectively) by measuring the absorbance at 275 nm; (iii) we calculated the observed octanol-water equilibrium constant (K_{OW}^{obs}) by employing Equation S6;

$$K_{OW}^{obs} = \frac{[Ar-SO_2NH_2]_W}{[Ar-SO_2NH_2]_O} \quad \text{(S6)}$$

and (iv) we corrected K_{OW}^{obs} for ionization of **BTA** in water by employing Equation S7, where $\theta_{Ar\text{-}SO2\text{-}NH2}$ is the fraction of protonated **BTA**.

$$K_{ow} = \theta_{Ar-SO2-NH2} \cdot K_{OW}^{obs} \quad \text{(S7)}$$

where

$$\theta_{Ar-SO2-NH2} = \frac{1}{1+10^{pH-pKa(Ar-SO2-NH2)}} \quad \text{(S8)}$$

Equation S7 is based on the assumption that **BTA** ionizes exclusively in the aqueous phase. In Equation S8, the pK_a of the sulfonamide group of **BTA** was adjusted for different buffer solutions in as described above.

To estimate $\Delta H°_{ow}$, we carried out the following steps: (i) we prepared 800 mL stock solutions consisting of 400 mL octanol + 400 mL buffer (10 mM sodium phosphate, 100 mM sodium salt, *pH* 7.8), and we placed these on a shaker for 24 hours; (ii) we measured $\Delta H°^{obs}_{dissolution}$ for **BTA** in buffer-saturated octanol and in octanol-saturated water ($n \geq 3$ for each medium in the presence of each salt) by following the experimental procedure outlined by Snyder et al;[2] (iii) we estimated the enthalpies of dissolution of the protonated form of BTA ($\Delta H°_{O,dissolution}$ for octanol, $\Delta H°_{W,dissolution}$ for water) by employing Eqs. S9and S10, where $\theta_{Ar\text{-}SO2\text{-}NH\text{-}}$ is the fraction of unprotonated **BTA**, $\Delta H°_{ion,Ar-SO2-NH2}$ is the enthalpy of ionization of the unionized form of **BTA**, and $\Delta H°_{ion,H2PO4-}$ is the enthalpy of ionization of $H_2PO_4^-$.

$$\Delta H°_{O,dissolution} = \Delta H°^{obs}_{O,dissolution} \quad \text{(S9)}$$

$$\Delta H°_{W,dissolution} = \Delta H°^{obs}_{W,dissolution} - \theta_{Ar-SO2-NH^-}\left(\Delta H°_{ion,Ar-SO2-NH2} - \Delta H°_{ion,H2PO4^-}\right) \quad \text{(S10)}$$

where

$$\theta_{Ar-SO2-NH^-} = \frac{1}{1+10^{pKa(Ar-SO2-NH^-)-PH}} \quad \text{(S11)}$$

Equation S9 is based on the assumption that **BTA** does not ionize in the octanol phase. Equation S10 corrects $\Delta H°^{obs}_{W,dissolution}$ for the enthalpy generated by the transfer of a proton from the sulfonamide of **BTA** to HPO_4^{2-}. In Equation S11, the pK_a of the sulfonamide group of **BTA** was adjusted for different buffer solutions as described above; (iv) finally, we estimated $\Delta H°_{ow}$ by employing Equation S12:

$$\Delta H°_{OW} = \Delta H°_{O,dissolution} - \Delta H°_{W,dissolution} \quad \text{(S12)}$$

Using estimated values of $\Delta G°_{ow}$ and $\Delta H°_{ow}$, we calculated values of $-T\Delta S°_{ow}$ in the presence of each salt. All values are reported in Table S5 and plotted in Figure S2. At concentrations of 100 mM, sodium salts of various anions did not significantly alter estimated

values of $\Delta H°_{ow}$ or $-T\Delta S°_{ow}$, and, for most salts $\Delta G°_{ow}$ ($P < 0.01$); Na_2SO_4, NaH_2PO_4, and $NaClO_4$ altered $\Delta G°_{ow}$ slightly (e.g. $\Delta\Delta G°_{ow} = \Delta G°_{ow}(Na_2HPO_4) - \Delta G°_{ow}(NaH_2PO_4) = -0.34$), but the absence of any trend in changes in $\Delta G°_{ow}$ along the Hofmeister series suggests that these changes could be the result of experimental error. The negligible influence of ions on the thermodynamics of the partitioning of **BTA** from buffer to octanol suggests that Equations 1 and 2 are valid.

Protein Crystallization and Ion Soaking. Monoclinic crystals of HCAII were prepared by a hanging drop vapor diffusion method.[9] Briefly, we carried out the following steps: (i) we prepared a concentrated solution of HCAII (~800 μM HCAII, 50 mM Tris-sulfate, *pH* 8.0) and a crystallization medium (1.15 M sodium citrate, 100 mM Tris-HCl, *pH* 7.8, hereafter referred to as "mother liquor"); (ii) we mixed 2-3 μL of protein solution with 2 μL of mother liquor within a single drop on the surface of a reservoir cover (EasyXtal CrystalSupport, Qiagen); (iii) we added 1 mL of mother liquor to a clear plastic reservoir in a 15-well plate (EasyXtal, Qiagen); (iv) we attached the reservoir cover to the reservoir, and we left the entire setup at 4°C.

We soaked the crystals of HCAII with anions by carrying out the following steps: (i) we prepared soaking solutions containing 1.32 M sodium citrate, 1 mM $ZnSO_4$, 100 mM Tris-HCl (*pH* 7.8), and 100 mM sodium salt (NaSCN, $NaClO_4$, NaI, or NaBr); (ii) within a single drop on the surface of a reservoir cover (EasyXtal CrystalSupport, Qiagen), we added 4 μL of soaking solution and 1-2 crystals of HCAII (picked via crystal loops from the crystallization droplets); (iii) to a clear plastic reservoir in a 15-well plate (EasyXtal, Qiagen), we added 1 mL of soaking solution; (iv) we attached the reservoir cover to the reservoir and left the entire setup at 4°C. We carried out soaking for ~1 week.

X-ray Crystallography. We collected X-ray diffraction data by using beam X-25 and the ADSC Quantum Q315 CCD detector at the National Synchrotron Light Source (Brookhaven National Laboratory, in collaboration with the Mail Program).[10] For each crystal, we collected diffraction data under a stream of liquid nitrogen (i.e., cryo-cooled). Reflections were indexed and integrated using HKL2000, and scaled using SCALEPACK.[11]

Solution of Crystal Structures. We analyzed diffraction data using the CCP4i suite of crystallography software and previously published procedures.[12] Table S7 summarizes the crystallographic details for each protein-ligand structure.

To determine the extent to which sodium salts distorted crystal packing by partially dehydrating protein crystals, we used PyMol to align each of our solved structures (i.e., HCAII complexed with SCN^-, ClO_4^-, I^-, and Br^-) with 3RYY. The RMSDs of aligned structures ranged from 0.085 to 0.157 Å, indicating that salts did not cause significant structural deviations between crystals.

WaterMap Calculations. We prepared the crystal structure of HCAII (www.rcsb.org; PDB entry 3RYY)[13] for WaterMap calculations by using the Protein Preparation Wizard[14] in Maestro (Maestro, version 9.7, Schrödinger, LLC, New York, NY, 2014) to add hydrogens, assign bond orders, optimize hydrogen bonding groups not unambiguously defined by the electron density (terminal rotamers of Asn, Gln, and His), predict optimal tautomers and ionization states, and optimize the hydrogen bonding network. We then performed a final minimization using the impref refinement module of IMPACT[15] with default settings. To focus our study on rearrangements of water triggered by the binding of anions to Zn^{2+} (as opposed to differences in arrangements of water caused by minor structural differences [RMSD of < 0.5 Å] between

anion-HCAII structures), we used the same protein structure coordinates for all calculations (3RYY, prepared following the procedure described above), and separately added each Hofmeister anion to this structure to create a new HCAII-anion complex. We carried out the following steps: (i) we superimposed the crystal structure of each HCAII-anion complex onto the template structure 3RYY by using the Protein Structure Alignment module in Maestro. Structures used for HCAII-anion complexes are as follows: SO_4^{2-} (2CBD), Ac^- (1XEG), Cl^- (1RAZ docked according to bromide), Br^- (this study), NO_3^- (1CAN), I^- (this study), ClO_4^- (this study), and SCN^- (this study). (ii) we swapped the ion from the HCAII-anion complex to the template structure; (iii) we used zero-order bonds both to restrain the negatively charged ions to their starting geometry with respect to the Zn^{2+} cofactor, and to restrain the Zn^{2+} cofactor to the protein; and (iv) we subjected each newly generated protein-anion complex to the molecular dynamics simulations described below.

For each anion-HCAII complex, we carried out WaterMap calculations as described previously.[16–18] Briefly, we performed molecular dynamics simulations using the Desmond MD engine[19] with the OPLS2005 force field.[20–22] The protein-anion complex was solvated with a TIP4P water box extending at least 10.0 Å beyond the protein in all directions and the default Desmond relaxation protocol was used; this protocol involves successive stages of constrained minimization followed by gradual heating to the final temperature of 300 K. After the relaxation step, we performed a 2.0-ns production MD simulation at a temperature of 300 K and pressure of 1 atm with positional restraints (5 kcal/mol/A^2) on the protein non-hydrogen atoms, extracted molecules of water from 7000 equally spaced snapshots, and subsequently clustered these molecules into distinct hydration sites. We computed the excess enthalpy (ΔH_{WM}) of water within each hydration site by taking the difference between (i) the average non-bonded interaction energy of waters in each hydration site from the HCAII-anion MD simulation and (ii) the

analogous quantity in the bulk fluid. We computed the excess entropy ($-T\Delta S_{WM}$) of water occupying each hydration site by using inhomogeneous solvation theory.[23,24] We computed the free energy (ΔG_{WM}) by summing excess enthalpy and entropy.

To score each protein-anion system, we summed the energies of all hydration sites within a specified radius from the Zn-bound anion. The computed values of $\Delta J°_{WM}$ (where $J = H$, TS, or G) represent the difference of thermodynamic properties of all waters within the integration radius in anion-bound and anion-free binding pockets ($\Delta J°_{WM,anion} = \Delta J°_{WM,HCA\text{-}anion} - \Delta J°_{WM,HCA}$). The quantity $\Delta J°_{WM,anion}(d)$ represents the $\Delta J°_{WM,anion}$ calculated by using waters beyond d Å from the Zn-bound anion in both the anion-HCAII and anion-free complexes (in the anion-free complexes, we summed the thermodynamic contribution of waters beyond specified distances from where the ion would be if the HCAII-anion complex was superimposed).

Appendix 1. The Hofmeister Series.

The Hofmeister series is a qualitative ranking of ions based on their tendency to precipitate proteins from aqueous solution (Figure 1A). Since its development, numerous studies have linked this series to a wide range of physical phenomena[25] (e.g., the tendency of ions to promote protein crystallization,[26] to prevent the hydrophobic collapse of polymers,[27] to drive colloidal assembly,[28] to activate enzymes in nonaqueous media,[29] and to trigger sol-gel transitions[30]). Despite their seemingly ubiquitous influence, however, Hofmeister effects—or specific ion effects (as opposed to nonspecific or Coulombic effects)—remain poorly understood on a molecular level.[31,32]

Recent evidence suggests that Hofmeister effects arise from direct interactions between ions and macromolecules, and between ions and the first solvation shells of those macromolecules;[8,33–37] ions, by perturbing the net charge and/or solvation structure of

macromolecular surfaces, alter the thermodynamics of intramolecular and intermolecular assembly. This mechanism is supported by (i) spectroscopic and thermodynamic studies showing that ions have a negligible influence on the structure of bulk water,[38,39] (ii) molecular dynamics simulations evidencing ion-specific binding sites on the surfaces of proteins and protein-like polymers,[40–42] and (iii) biophysical studies showing a correlation between the influence of ions on the stability of polymeric structures and the tendency of those ions to polarize molecules of water, to order water at interfaces, or to enhance the free energetic cost associated with hydrating hydrophobic surfaces.[27,43–45] Despite an emerging consensus that Hofmeister effects arise from interfacial phenomena, however, the specific ion-macromolecule and ion-water interactions in which ions engage at interfaces—and the thermodynamic mechanisms underlying those interactions—have proven difficult to examine directly and, thus, remain the subject of substantial controversy.[31,32,46]

Appendix 2. Ion Pairs and the "Law of Matching Water Affinities"

In solution, the association of two small, strongly hydrated ions—a process that often results in the entropically favorable transfer of molecules of water from the solvation shells of those ions to bulk water—can be entropically favorable or unfavorable, depending on the entropic cost of forming an ion pair;[47,48] by contrast, the association of large, weakly hydrated ions, which often results in the entropically unfavorable transfer of "mobile" molecules of water from the solvation shells of those ions, tends to be entropically unfavorable.[47] Regardless of the overall sign of the entropic contribution, however, the formation of ion pairs in aqueous solution tends to be dominated by the enthalpic term.[47,49]

In accordance with the aforementioned discussion, the Law of Matching Water Affinities can be discussed (and often is discussed) in the context of enthalpy.[42,46,49–52] In this context, the

theory suggests that two ions associate with one another when the enthalpic cost of partially desolvating those ions is more than compensated by the enthalpic benefit of either (i) forming an ion pair (for small, strongly hydrated ions that engage in ion-water interactions that are more enthalpically favorable than water-water interactions) or (ii) water-water interactions (for large, weakly hydrated ions that engage in ion-water interactions that are less enthalpically favorable than water-water interactions).

Appendix 3. Iodide in the binding pocket

In the main text, we refer to the binding sites of iodide in order of their proximity to the Zn^{2+} cofactor (I-1 through I-4, closest to farthest away) (Figures 2B-2D). I-1 and I-2 (positioned 2.4 Å and 3.8 Å, respectively, from Zn^{2+}, and 1.7 Å from one another) denote alternative binding sites for ion-Zn complexation, and are not occupied simultaneously; these sites likely permit the formation of an inner-sphere ion pair (one that involves ion-ion contact) and an outer-sphere ion pair (one that involves a shared solvating water), respectively. I-3 (positioned 5.7 Å away from Zn^{2+}) denotes a binding site at the border of the hydrophilic and hydrophobic surfaces (Figure 3B); it sits in close proximity (3.5 Å) to the amine of Gln-92. Its distance from the I-2 site (3.7 Å) suggests that iodide does not occupy the I-2 and I-3 sites simultaneously. I-4 (positioned 11.9 Å away from Zn^{2+} and 6.8 Å from I-3; Fig 3D) denotes a binding site within a small hydrophobic declivity formed by five nonpolar side chains near the mouth of the binding pocket (Figures 3B and 3D). When the I-2 site is not occupied, the binding pocket of HCAII can hold three iodides (I-1, I-3, and I-4); when the I-2 site is occupied, the binding pocket can hold two iodides (I-2 and I-4).

Appendix 4. Charges in the I-4 Binding Pocket

The I-4 binding site comprises a hydrophobic declivity in the wall of the binding pocket of HCAII. Although there are no positively charged side chains within 5 Å of the iodide bound to this declivity (Figure 3B), the nonpolar residues could support a positive charge. To examine charges on the surface of HCAII in the vicinity of the I-4 site, we employed the Adaptive Poisson-Boltzmann Solver (APBS)[53] software package for PyMOL to map the electrostatic surface of the protein (Figure S4). The I-4 declivity shows some positive charge (light blue), but that charge is small compared to positive charges (intense blue regions) located elsewhere on the surface (where iodide does not bind); this result suggests that Coulombic attraction is not the primary driving force for the association of iodide with the I-4 site.

SI Figures

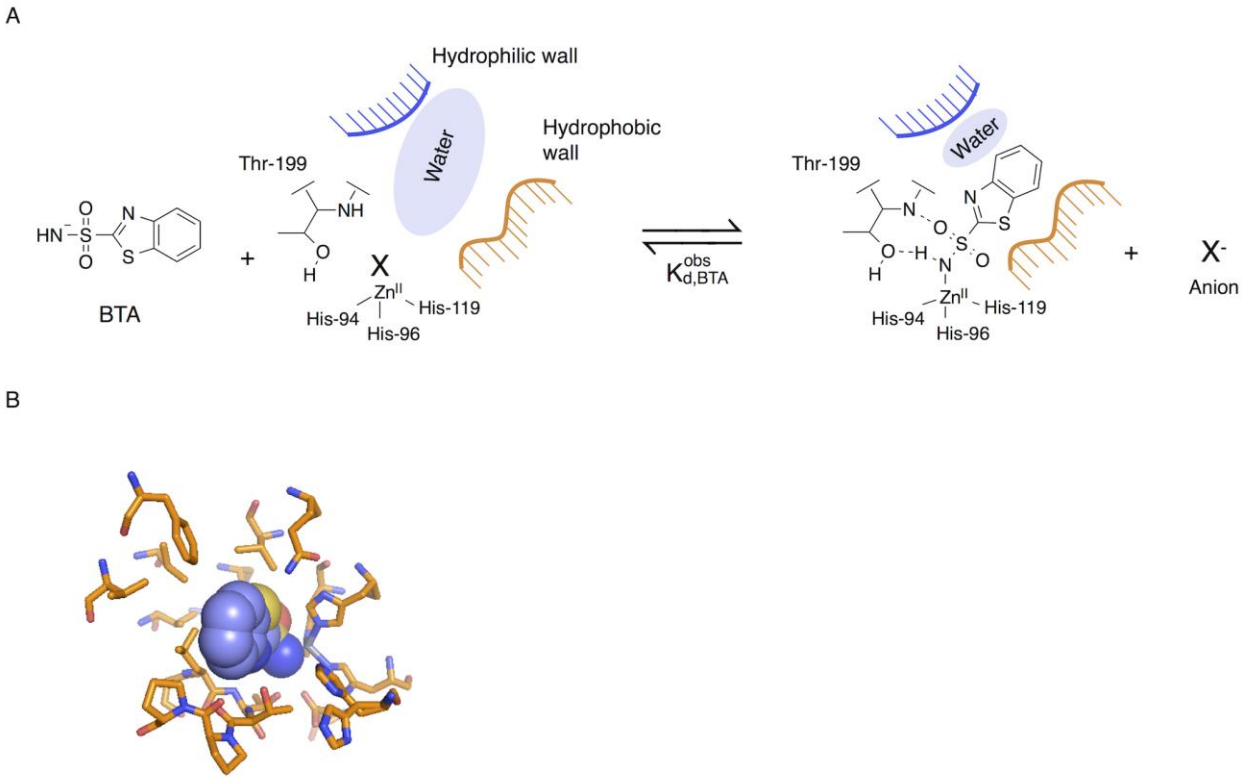

Figure S1. The competition assay. (A) The binding of deprotonated **BTA** to HCAII displaces Zn^{2+}-bound anions, permitting the estimation of $K_{d,\ anion}$ and $\Delta H°_{bind,anion}$ from known values of $K_{d,\ BTA}$ and $\Delta H°_{bind,BTA}$ and observed values of $K_{d,BTA,obs}$ and $\Delta H°_{bind,BTA,obs}$ (measured in the presence of the anions). (B) Structure o the active site of HCAII complexed with **BTA** (PDB entry 3S73).

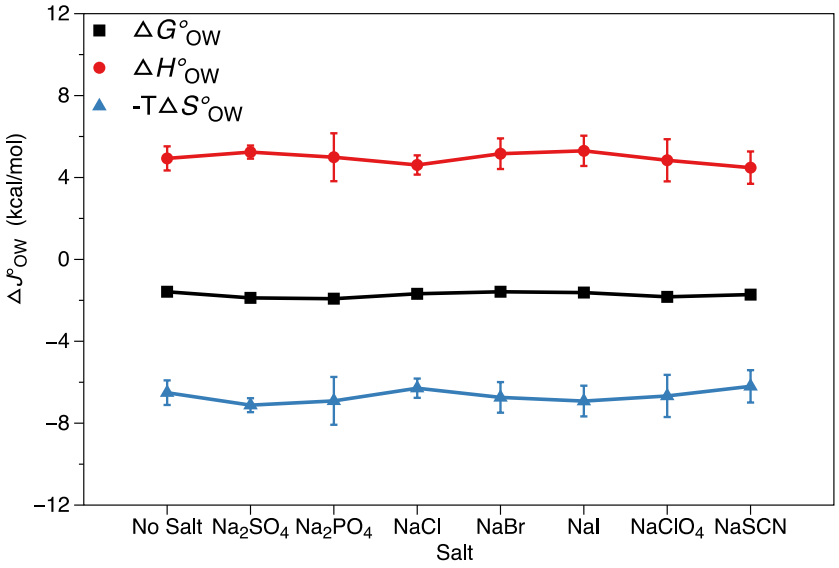

Figure S2. Estimated thermodynamic parameters for the partitioning of BTA from buffer to octanol. At concentration of 100 mM, sodium salts with anions spanning the Hofmeister series exhibit no statistically significant influence on the thermodynamics of BTA partitioning between water and octanol; this result suggests that salts (at concentrations of 100 mM), in the context of BTA binding to HCAII, do not influence the thermodynamics of BTA desolvation.

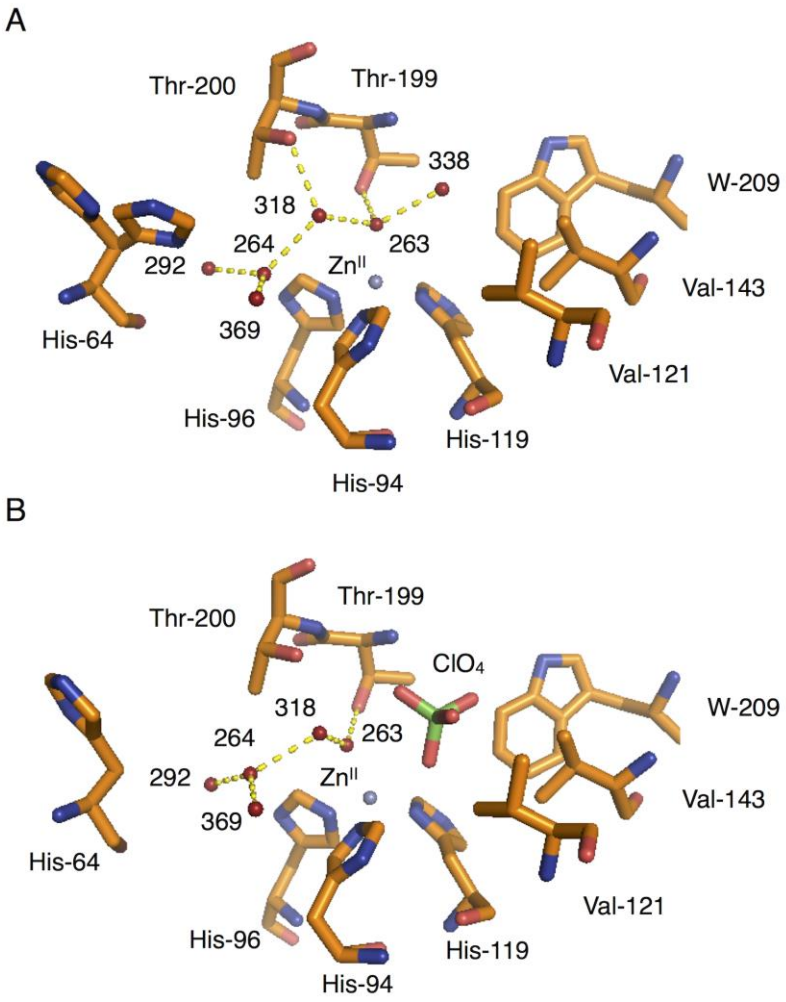

Figure S3. Structural basis of anion binding. (A) X-ray crystal structure of the active site of HCAII (PDB entry 2CBA) showing six waters, each of which contributes either directly or indirectly to catalysis. (B) X-ray crystal structure of the active site of HCAII complexed with ClO_4^-. Both ClO_4^- and SCN^- displace H_2O-338 (the "so-called" deep water) and shift the position of H_2O-263 (the catalytically important Zn-bound water).

A

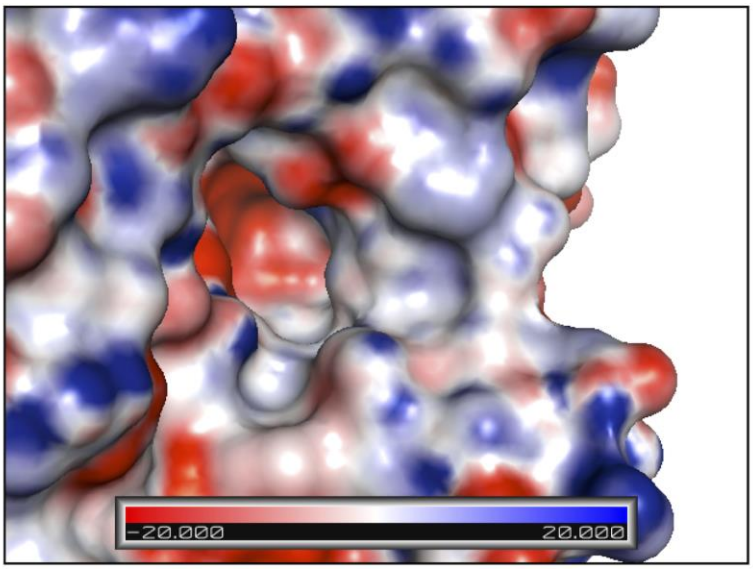

B

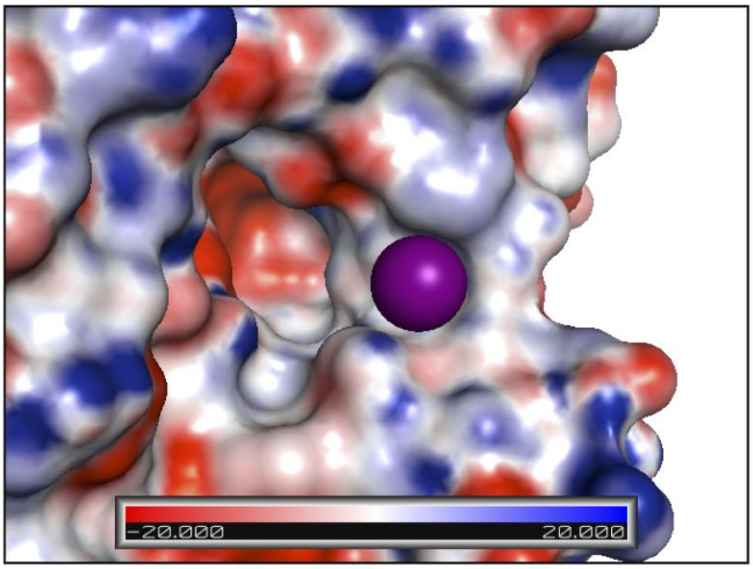

Figure S4. Electrostatics near the I-4 binding site. (A-B) A color-coded electrostatic surface (the protein/water contact surface) of HCAII in the vicinity of the I-4 binding site (units of K_bT/e_c): (A) without and (B) with the iodide present (shown as a sphere indicating the ion/water contact surface). Although the I-4 declivity shows some positive charge (light blue), that charge is small compared to larger positive charges (intense blue) located elsewhere on the protein, suggesting that Coulombic attraction is not the primary driving force for the binding of iodide to the I-4 site.

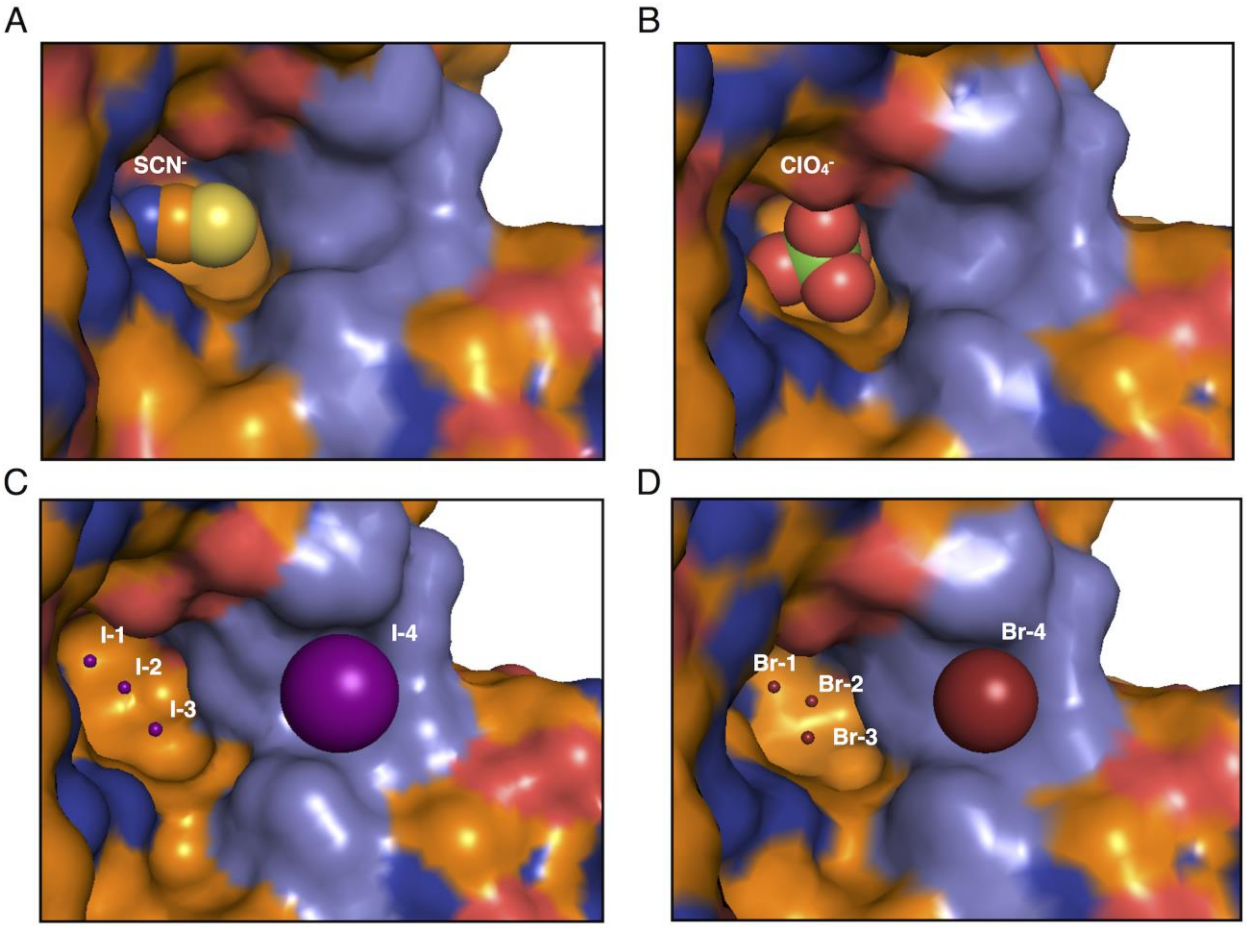

Figure S5. The influence of ion shape on the affinity of ions for the I-4 binding site. X-ray crystal structures of HCAII complexed with (A) thiocyanate (SCN^-, PDB entry 4YGK), (B) perchlorate (ClO_4^-, PDB entry 4YGL), (C) iodide (I^-, PDB entry 4YGN), and (D) bromide (Br^-, PDB entry 4YGJ) ions. In (C-D), ions are labeled according to their distance from the Zn^{2+} cofactor. Sites 1 and 2 denote alternative binding sites for the Zn-bound anion (an inner-sphere ion pair and an outer-sphere ion pair, respectively). Site 3 denotes a binding site at the border of the hydrophobic and hydrophilic surfaces. Site 4 denotes a binding site in the hydrophobic wall. Anions in site 4 are shown as spheres that indicate the ion/water contact surface; the surface of the protein is represented similarly. A comparison of (A-D) suggests that only spherical anions can bind the hemisphere-shaped I-4 binding site.

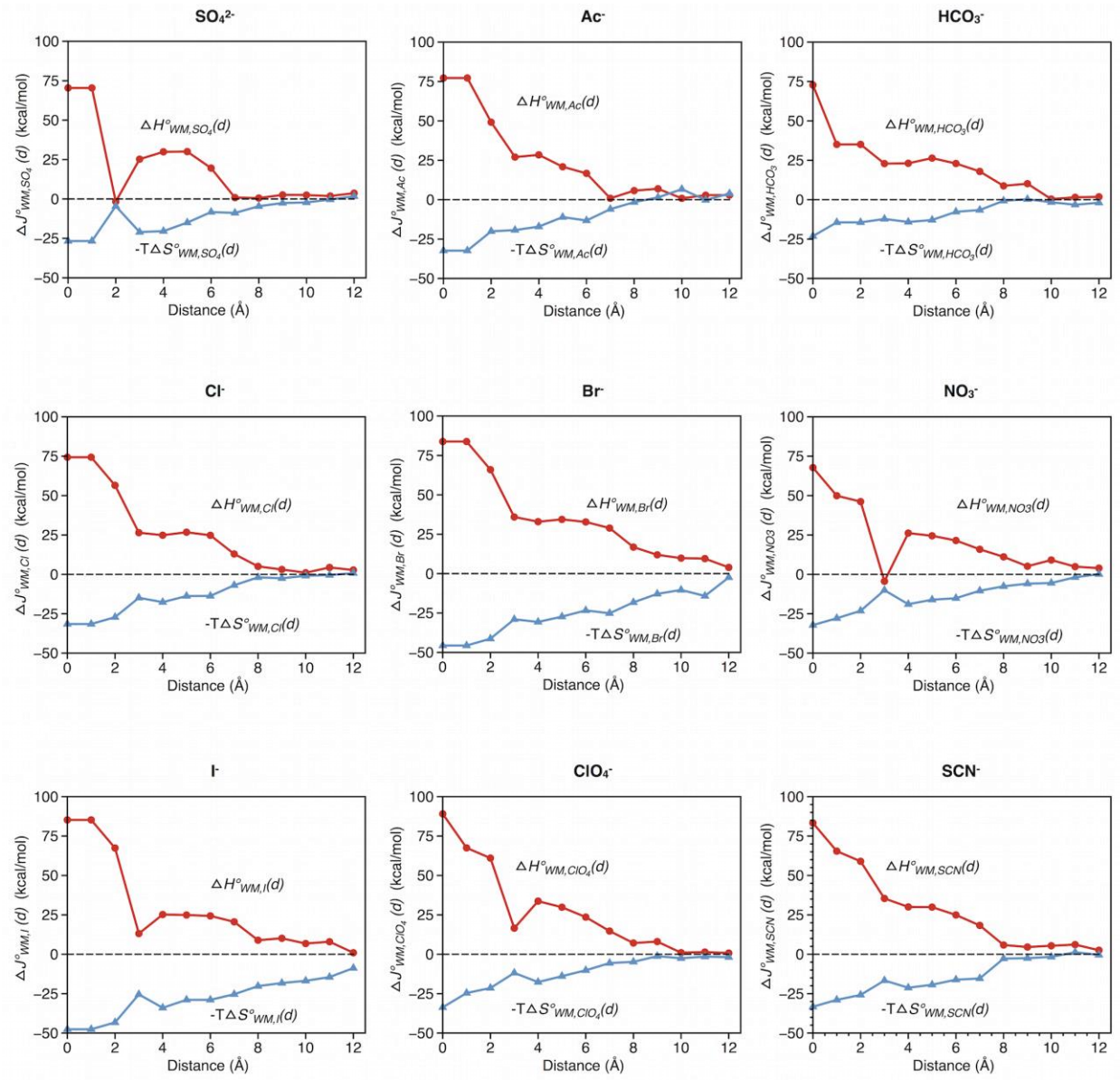

Figure S6. The length scales of rearrangements of water triggered by the formation of ion pairs between anions and the Zn^{2+} cofactor. Plots show values of $\Delta H°_{WM\text{-}anion}(d)$ and $-T\Delta S°_{WM\text{-}anion}(d)$ for the formation of ion pairs between anions and Zn^{2+}, calculated by summing over waters beyond a certain distance *d* Å from the surface of the bound anion. This plot suggests that anions triggers rearrangements of water that extend up to ~8 Å from their surfaces.

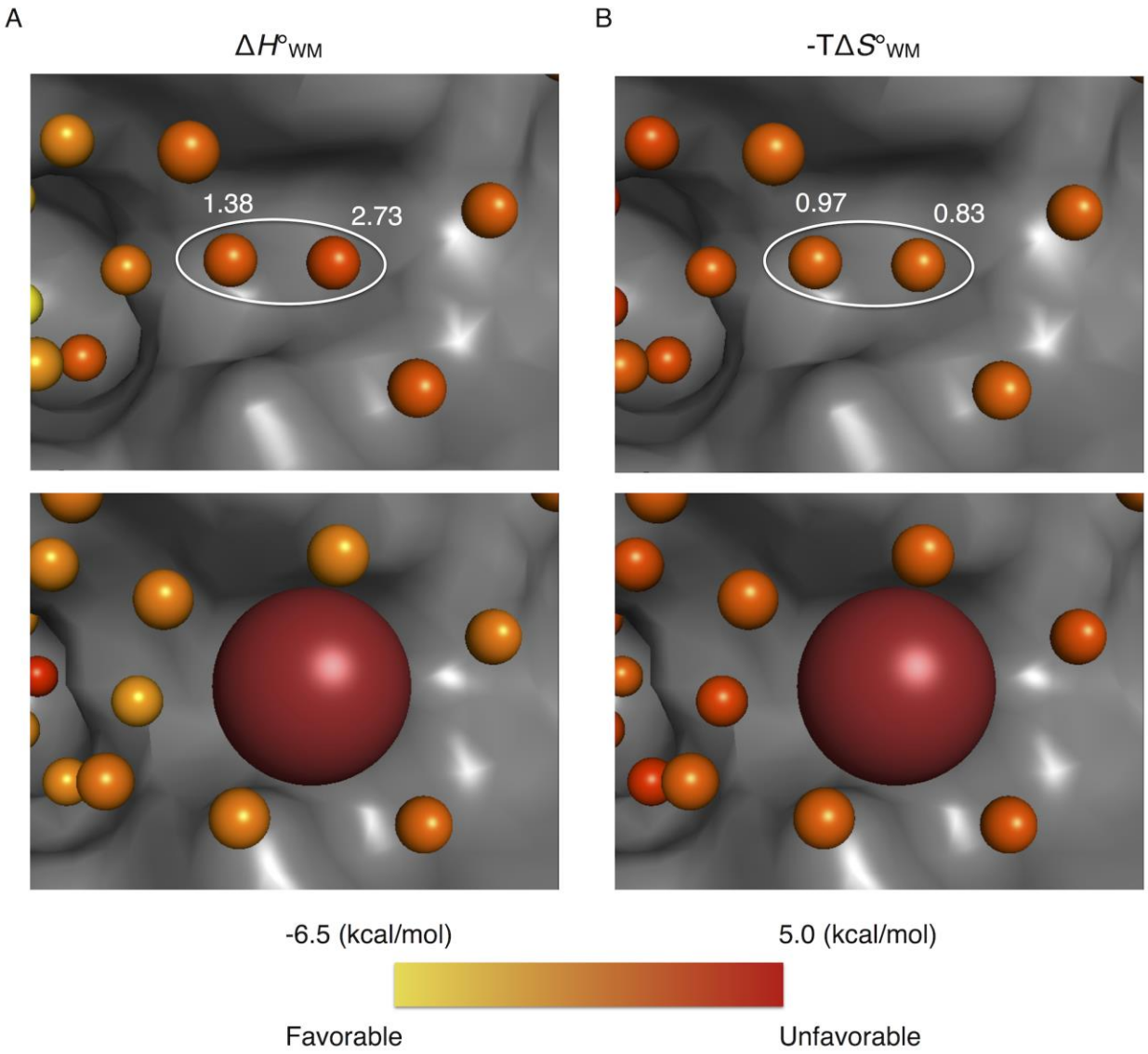

Figure S7. Rearrangements of water triggered by the association of bromide with the I-4 binding pocket. (A-B) WaterMap results for bromide in the I-4 binding pocket: (top) without bromide bound and (bottom) with bromide bound. Waters are colored according to (A) their enthalpies ($\Delta H°_{WM}$) and (B) their entropies ($-T\Delta S°_{WM}$), relative to bulk water. In all images, the surface of the protein appears in gray. Results suggest that the binding of bromide to the I-4 binding pocket causes displacement of two enthalpically and entropically unstable (relative to bulk water) molecules of water (circled and labeled with their corresponding thermodynamic quantities).

Tables

Table S1. Observed thermodynamic binding parameters.

Ligand	*Ion*	*Samples*	*n*	$K_{d,BTA}^{obs-ITC}$ *(nM)*	$\Delta G^{\circ}{}_{bind,BTA}^{obs-ITC}$ *(kcal/mol)*	$\Delta H^{\circ}{}_{bind,BTA}^{obs-ITC}$ *(kcal/mol)*	$-T\Delta S^{\circ}{}_{bind,BTA}^{obs-ITC}$ *(kcal/mol)*
BTA	n/a	23	0.98	4.4 (2.1)	-11.47 (0.30)	-16.44 (0.74)	4.97 (0.87)
BTA	$SO4^{2-}$	9	0.97	1.5 (0.5)	-12.06 (0.21)	-15.67 (0.43)	3.61 (0.42)
BTA	$H_2PO_4^-$	9	1.06	4.2 (2.4)	-11.50 (0.28)	-14.93 (0.52)	3.43 (0.78
BTA	Ac^-	13	1.03	10.9 (3.4)	-11.00 (0.24)	-14.51 (1.30)	3.51 (1.43)
BTA	HCO_3^-	12	1.00	7.0 (1.3)	-11.13 (0.11)	-17.41 (0.70)	6.32 (0.77)
BTA	Cl^-	7	0.98	19.4 (2.0)	-10.53 (0.06)	-14.71 (0.37)	4.19 (0.36)
BTA	Br^-	7	1.02	22.1 (2.8)	-10.45 (0.08)	-12.67 (0.36)	2.22 (0.39)
BTA	NO_3^-	7	0.97	44.6 (5.0)	-10.03 (0.07)	-8.77 (0.59)	-1.26 (0.62)
BTA	I^-	7	0.97	33.9 (6.8)	-10.20 (0.12)	-9.41 (0.10)	-0.79 (0.19)
BTA	ClO_4^-	7	1.02	113.9 (36.1)	-9.51 (0.24)	-3.77 (0.19)	-5.74 (0.38)
BTA	SCN^-	7	0.93	86.3 (18.9)	-9.65 (0.13)	-7.04 (0.26)	-2.61 (0.38)

*Errors represent standard deviation ($n \geq 7$).

Table S2. pK_a-corrected thermodynamic binding parameters.

Ligand	*Ion*	K_d *(nM)*	$-\Delta G^\circ$ *(kcal/mol)*	$-\Delta H^\circ$ *(kcal/mol)*	$-T\Delta S^\circ$ *(kcal/mol)*
BTA	n/a	0.15 (0.07)	-13.48 (0.30)	-16.63 (0.74)	3.15 (0.87)
BTA	$SO4^{2-}$	0.09 (0.03)	-13.78 (0.21)	-14.82 (0.43)	0.42 (0.14)
BTA	HPO_4^{2-}	0.20 (0.11)	-13.29 (0.28)	-14.54 (0.52)	1.25 (0.78)
BTA	Ac^-	0.47 (0.14)	-12.86 (0.24)	-14.24 (1.30)	1.38 (1.43)
BTA	HCO_3^-	0.32 (0.06)	-12.96 (0.11)	-17.35 (0.70)	4.39 (0.77)
BTA	Cl^-	0.83 (0.09)	-12.39 (0.06)	-14.54 (0.37)	2.14 (0.36)
BTA	Br^-	0.95 (0.12)	-12.31 (0.08)	-12.49 (0.36)	0.18 (0.39)
BTA	NO_3^-	1.91 (0.21)	-11.90 (0.07)	-8.59 (0.59)	-3.31 (0.62)
BTA	I^-	1.45 (0.29)	-12.07 (0.12)	-9.23 (0.10)	-2.84 (0.19)
BTA	ClO_4^-	4.88 (1.55)	-11.37 (0.24)	-3.59 (0.19)	-7.78 (0.38)
BTA	SCN^-	3.70 (0.81)	-11.52 (0.13)	-6.86 (0.26)	-4.66 (0.38)

*Errors represent standard deviation ($n \geq 7$).

Table S3. Estimated values of the pK_a of the sulfonamide group of BTA under various buffer conditions.

Ligand	*Sodium Salt**	***I* (M)**	pK_a
BTA	n/a	0.02	8.2
BTA	Na_2SO4	0.32	7.95
BTA	Na_2HPO_4	0.22	7.99
BTA	NaAc	0.12	8.06
BTA	$NaHCO_3$	0.11	8.06
BTA	NaCl	0.12	8.06
BTA	NaBr	0.12	8.06
BTA	$NaNO_3$	0.12	8.06
BTA	NaI	0.12	8.06
BTA	$NaClO_4$	0.12	8.06
BTA	NaSCN	0.12	8.06
HCAII	n/a	n/a	6.9

*10 mM sodium phosphate (*pH* 7.6) with 100 mM of the indicated sodium salt. Sodium salts, as shown, indicate the dominant anion present in solution at *pH* = 7.6: HPO_4^{2-} (72% of total phosphate species) and $H_2PO_4^-$ (28%); HCO_3^- (95%) and H_2CO_3 (5%); all other anions (100%).

Table S4. Estimated thermodynamic parameters for ions.

Ion	K_d *(mM)*	$-\Delta G^\circ$ *(kcal/mol)*	$-\Delta H^\circ$ *(kcal/mol)*	$-T\Delta S^\circ$ *(kcal/mol)*
Ac^-	46.2 (8.9)	-1.82 (0.11)	-3.21 (0.46)	1.39 (0.48)
HCO_3^-	84.2 (17.5)	-1.47 (0.12)	1.68 (0.37)	-3.14 (0.39)
Cl^-	21.6 (2.8)	-2.27 (0.08)	-2.32 (0.22)	0.05 (0.23)
Br^-	18.5 (2.4)	-2.36 (0.08)	-4.68 (023)	2.31 (0.24)
NO_3^-	8.4 (1.0)	-2.83 (0.07)	-8.51 (0.28)	5.67 (0.29)
I^-	11.3 (1.6)	-2.66 (0.08)	-8.03 (0.19)	5.37 (0.21)
ClO_4^-	3.1 (0.5)	-3.42 (0.10)	-13.25 (0.18)	9.83 (0.20)
SCN^-	4.2 (0.6)	-3.25 (0.08)	-9.98 (0.19)	6.73 (0.20)

*Errors represent standard error ($n \geq 7$) as in Figure 2.

Table S5. Estimated thermodynamic parameters for the partitioning of BTA from buffer to octanol in the presence of different sodium salts.

Salt (100 mM)	$-\Delta G^{\circ}$ *(kcal/mol)*	$-\Delta H^{\circ}$ *(kcal/mol)*	$-T\Delta S^{\circ}$ *(kcal/mol)*
No salt	-1.58 (0.08)	4.93 (0.59)	-6.51 (0.60)
Na_2SO_4	-1.88 (0.12)	5.24 (0.32)	-7.12 (0.34)
NaH_2PO_4	-1.92 (0.04)	4.99 (1.17)	-6.91 (1.17)
NaCl	-1.68 (0.08)	4.61 (0.47)	-6.29 (0.47)
NaBr	-1.58 (0.05)	5.16 (0.75)	-6.74 (0.75)
NaI	-1.62 (0.07)	5.30 (0.74)	-6.92 (0.75)
$NaClO_4$	-1.83 (0.08)	4.84 (1.03)	-6.67 (1.03)
NaSCN	-1.72 (0.05)	4.48 (0.79)	-6.20 (0.79)

*Errors represent standard deviation ($n \geq 6$).

Table S6. Properties of ions*.

Ion	Volume (cm^3 / mol)	$\Delta G^\circ_{hydration}$ (kcal/mol)	$\Delta H^\circ_{hydration}$ (kcal/mol)	Polarizability (cm^3 / mol)
$SO4^{2-}$	25	-261	-247	13.63
$H_2PO_4^-$	34.6	-113	-125	14.60
Ac^-	46.2	-89	-102	13.82
HCO_3^-	28.9	-88	-92	10.90
Cl^-	23.3	-83	-88	8.57
Br^-	30.2	-77	-80	12.22
NO_3^-	34.5	-73	-75	10.59
I^-	41.7	-68	-70	18.68
ClO_4^-	49.6	-51	-59	12.89
SCN^-	41.2	-69	-74	17.33

*All data taken from Marcus.[54]

Table S7. Crystallography data for the anion-HCAII complexes

	ClO_4^-	SCN^-	I^-	Br-
Data collection and processing				
No. crystals analyzed	1	1	1	1
Wavelength	1.100 Å	1.100 Å	1.100 Å	0.91 Å
Space group	$P2_1$	$P2_1$	$P2_1$	$P2_1$
Unit cell parameters				
a	42.138	42.391	42.341	42.30
b	41.04	41.346	41.336	41.38
c	72.878	72.912	72.837	72.46
α	90	90	90	90
β	104.45	104.7	104.6	104.6
γ	90	90	90	90
Diffraction data				
High resolution bin	1.549-1.510	1.54-1.50	1.261-1.229	1.129-1.100
# of reflections	2440	2400	1921	5792
Refinement				
Resolution range	40-1.51	50-1.50	50-1.23	50-1.1
Completeness	98.2	95.2	87.9	84.13
R(work)	0.187	0.173	0.175	0.123
R(free)	0.213	0.213	0.209	0.143
B(avg)	11.3	10.0	14.7	14.2
Bond lengths	0.027	0.021	0.022	0.024
Bond angles	2.55	2.11	2.16	2.35
Protein residues	257	257	256	258
Zinc ions	1	1	1	1
Water molecules	218	232	142	269
Anion (inhibitor) atoms	15	3	5	10

SI References:

(1) Christianson, D. W.; Fierke, C. A. *Acc. Chem. Res.* **1996**, *29*, 331.

(2) Snyder, P. W.; Mecinovic, J.; Moustakas, D. T.; Thomas, S. W.; Harder, M.; Mack, E. T.; Lockett, M. R.; Heroux, A.; Sherman, W.; Whitesides, G. M. *Proc. Natl. Acad. Sci. U. S. A.* **2011**, *108*, 17889.

(3) Breiten, B.; Lockett, M. R.; Sherman, W.; Fujita, S.; Al-Sayah, M.; Lange, H.; Bowers, C. M.; Heroux, A.; Krilov, G.; Whitesides, G. M. *J. Am. Chem. Soc.* **2013**, *135*, 15579.

(4) Goldberg, R. N.; Kishore, N.; Lennen, R. M. *J. Phys. Chem. Ref. Data*, **2002**, *31*, 231.

(5) Stumm, W.; J., M. J. *Aquatic Chemistry: Chemical Equilibria and Rates in Natural Waters*; 3rd ed.; John Wiley & Sons, Inc.: Hoboken, NJ, **1996**;102.

(6) Chodera, J. D.; Mobley, D. L. *Annu. Rev. Biophys.* **2013**, *42*, 121.

(7) Zhang, Y. L.; Zhang, Z. Y. *Anal. Biochem.* **1998**, *261*, 139.

(8) Pegram, L. M.; Record, M. T. *J. Phys. Chem. B* **2008**, *112*, 9428.

(9) Rhodes, G. *Crystallography made crystal clear; a guide for users of macromolecular models*; 1st ed.; Academic Press: San Diego, CA, **1993**; 36.

(10) Robinson, H.; Soares, A. S.; Becker, M.; Sweet, R.; Héroux, A. *Acta Crystallogr. Sect. D Biol. Crystallogr.* **2006**, *62*, 1336.

(11) Otwinowski, Z.; Minor, W. *Methods Enzymol.* **1997**, *276*, 307.

(12) Bailey, S. *Acta Crystallogr. Sect. D Biol. Crystallogr.* **1994**, *50*, 760.

(13) Berman, H. M.; Westbrook, J.; Feng, Z.; Gilliland, G.; Bhat, T. N.; Weissig, H.; Shindyalov, I. N.; Bourne, P. E. *Nucleic Acids Res.* **2000**, *28*, 235.

(14) Madhavi Sastry, G.; Adzhigirey, M.; Day, T.; Annabhimoju, R.; Sherman, W. *J. Comput. Aided. Mol. Des.* **2013**, *27*, 221.

(15) Banks, J. L.; Beard, H. S.; Cao, Y.; Cho, A. E.; Damm, W.; Farid, R.; Felts, A. K.; Halgren, T. A.; Mainz, D. T.; Maple, J. R.; Murphy, R.; Philipp, D. M.; Repasky, M. P.; Zhang, L. Y.; Berne, B. J.; Friesner, R. A.; Gallicchio, E.; Levy, R. M. *J. Comp. Chem.* **2005**, *26*, 1752.

(16) Beuming, T.; Farid, R.; Sherman, W. *Protein Sci.* **2009**, *18*, 1609.

(17) Beuming, T.; Che, Y.; Abel, R.; Kim, B.; Shanmugasundaram, V.; Sherman, W. *Proteins Struct. Funct. Bioinforma.* **2012**, *80*, 871.

(18) Robinson, D. D.; Sherman, W.; Farid, R. *ChemMedChem* **2010**, *5*, 618.

(19) Bowers, K. J.; Chow, E.; Xu, H. X. H.; Dror, R. O.; Eastwood, M. P.; Gregersen, B. A.; Klepeis, J. L.; Kolossvary, I.; Moraes, M. A.; Sacerdoti, F. D.; Salmon, J. K.; Shan, Y. S. Y.; Shaw, D. E. *ACM/IEEE SC 2006 Conf.* **2006**.

(20) Kaminski, G. A.; Friesner, R. A.; Tirado-Rives, J.; Jorgensen, W. L. *J. Phys. Chem. B* **2001**, *105*, 6474.

(21) Jorgensen, W. L.; Maxwell, D. S.; Tirado-Rives, J. *J. Am. Chem. Soc.* **1996**, *118*, 11225.

(22) Shivakumar, D.; Williams, J.; Wu, Y.; Damm, W.; Shelley, J.; Sherman, W. *J. Chem. Theory Comput.* **2010**, *6*, 1509.

(23) Young, T.; Abel, R.; Kim, B.; Berne, B. J.; Friesner, R. A. *Proc. Natl. Acad. Sci. U. S. A.* **2007**, *104*, 808.

(24) Abel, R.; Young, T.; Farid, R.; Berne, B. J.; Friesner, R. A. *J. Am. Chem. Soc.* **2008**, *130*, 2817.

(25) Kunz, W.; Lo Nostro, P.; Ninham, B. W. *Cur. Opin. Col. Int. Science* **2004**; Vol. 9, 1.

(26) Ries-Kautt, M.; Ducruix, A. *Methods Enzymol.* **1997**, *276*, 23.

(27) Zhang, Y.; Furyk, S.; Bergbreiter, D. E.; Cremer, P. S. *J. Am. Chem. Soc.* **2005**, *127*, 14505.

(28) Filankembo, a.; Pileni, M. P. *J. Phys. Chem. B* **2000**, *104*, 5865.

(29) Ru, M. T.; Hirokane, S. Y.; Lo, A. S.; Dordick, J. S.; Reimer, J. A.; Clark, D. S. *J. Am. Chem. Soc.* **2000**, *122*, 1565.

(30) Lloyd, G. O.; Steed, J. W. *Nat. Chem.* **2009**, *1*, 437.

(31) Tobias, D. J.; Hemminger, J. C. *Science* **2008**, *319*, 1197.

(32) Jungwirth, P.; Cremer, P. S. *Nat. Chem.* **2014**, *6*, 261.

(33) Marcus, Y. *Chem. Rev.* **2009**, *109*, 1346.

(34) Zhang, Y.; Cremer, P. S. *Cur. Opin. Chem. Biol.* **2006**, *10*, 658.

(35) Zhang, Y.; Cremer, P. S. *Annu. Rev. Phys. Chem.* **2010**, *61*, 63.

(36) Pegram, L. M.; Wendorff, T.; Erdmann, R.; Shkel, I.; Bellissimo, D.; Felitsky, D. J.; Record, M. T. *Proc. Natl. Acad. Sci. U. S. A.* **2010**, *107*, 7716.

(37) Shimizu, S.; McLaren, W. M.; Matubayasi, N. *J. Chem. Phys.* **2006**, *124*.

(38) Omta, A. W.; Kropman, M. F.; Woutersen, S.; Bakker, H. J. *Science* **2003**, *301*, 347.

(39) Batchelor, J. D.; Olteanu, A.; Tripathy, A.; Pielak, G. J. *J. Am. Chem. Soc.* **2004**, *126*, 1958.

(40) Rembert, K. B.; Paterová, J.; Heyda, J.; Hilty, C.; Jungwirth, P.; Cremer, P. S. *J. Am. Chem. Soc.* **2012**, *134*, 10039.

(41) Vrbka, L.; Vondrásek, J.; Jagoda-Cwiklik, B.; Vácha, R.; Jungwirth, P. *Proc. Natl. Acad. Sci. U. S. A.* **2006**, *103*, 15440.

(42) Hess, B.; van der Vegt, N. F. A. *Proc. Natl. Acad. Sci. U. S. A.* **2009**, *106*, 13296.

(43) Gurau, M. C.; Lim, S. M.; Castellana, E. T.; Albertorio, F.; Kataoka, S.; Cremer, P. S. *J. Am. Chem. Soc.* **2004**, *126*, 10522.

(44) Zhang, Y.; Cremer, P. S. *Proc. Natl. Acad. Sci. U. S. A.* **2009**, *106*, 15249.

(45) Chen, X.; Yang, T.; Kataoka, S.; Cremer, P. S. *J. Am. Chem. Soc.* **2007**, *129*, 12272.

(46) Jungwirth, P.; Winter, B. *Annu. Rev. Phys. Chem.* **2008**, *59*, 343.

(47) Collins, K. D.; Neilson, G. W.; Enderby, J. E. *Biophys. Chem.* **2007**, *128*, 95.

(48) Cecchi, T. *Ion-Pair Chromatography and Related Techniques*; Taylor & Francis Group: Boca Raton, FL, 2010; 18.

(49) Collins, K. D. *Biophys. Chem.* **2006**, *119*, 271.

(50) Collins, K. D. *Biophys. J.* **1997**, *72*, 65.

(51) Collins, K. D. *Methods* **2004**, *34*, 300.

(52) Uejio, J. S.; Schwartz, C. P.; Duffin, A. M.; Drisdell, W. S.; Cohen, R. C.; Saykally, R. J. *Proc. Natl. Acad. Sci. U. S. A.* **2008**, *105*, 6809.

(53) Baker, N. A.; Sept, D.; Joseph, S.; Holst, M. J.; McCammon, J. A. *Proc. Natl. Acad. Sci. U. S. A.* **2001**, *98*, 10037.

(54) Marcus, Y. *Ion Properties*; Marcel Dekker: New York, New York, **1997**.